Magnetoconductance Oscillations of n-Type Inversion Layers in InSb Surfaces

Nobuo Kotera, Yoshifumi Katayama, and Kiichi F. Komatsubara
Central Research Laboratory, Hitachi Ltd., Kobubunji, Tokyo, Japan
(Received 7 September 1971)

The galvanomagnetic properties of conduction electrons in n-type inversion layers of InSb have been investigated. The motion of electrons in an inversion layer is quantized in the direction normal to the surface by the surface electric field associated with the inversion layer. In a strong magnetic field normal to the surface, the motion parallel to the surface is also quantized into Landau orbits. In such a condition, the conductance of the inversion layer was measured as a function of surface electric field and a Shubnikov–de Haas–type oscillation was observed. A change of the surface electric field results in a change of the density of conduction carriers and also in a change of the energy levels due to the above quantizations relative to the bulk Fermi level. The conductance oscillation is the result of the successive passage of Landau levels through the Fermi level. In the experiments, two series of conductance oscillations were observed, which are reasonably ascribed to the two series of Landau levels associated with the two quantized energy levels, i.e., the lowest and the next-to-lowest electric subbands. The observed oscillation pattern of the conductance was compared with the one deduced from a simple theoretical model, and a good agreement was found. Besides the Shubnikov–de Haas–type oscillation, other galvanomagnetic properties are also discussed.

I. INTRODUCTION

Electrons have three-dimensional freedom of motion. However, when these electrons are confined in a one-dimensional potential well whose width is smaller than the wavelength of the electrons, the motion of electrons is quantized in one dimension, and the motion in the other two dimensions is left free. Thus, the energy spectrum is given by the discrete levels for the one-dimensional quantization, each of which has a continuum for the two-dimensional free motion. In a strong magnetic field normal to the surface, the two-dimensional motion parallel to the surface is also quantized into Landau orbits. The energy spectrum of such an electron system is completely discrete, and many Landau levels are associated with each one-dimensionally quantized state.

In such a system, the electrons do not have any average velocity in the direction of the electric field applied perpendicular to the magnetic field, preventing them from carrying the electrical current in the direction of the applied electric field in an ideal case. However, they are able to carry the electrical current as a result of scatterings. That is, the center of the Landau orbit jumps in the direction of the electric field with the aid of scatterings. Because the probability of such scatterings is large where the density of states of the carriers is large, the electrical conductivity would be related to the energy spectra of the conduction carriers. In contrast to our case, note that in the usual transport phenomenon, the scattering of carriers acts as a resistance to the electrical current.

With the recent progress of semiconductor technology, it has become possible to make use of the semiconductor surface as a narrow one-dimensional potential well of conduction electrons. The transport phenomena of such one-dimensionally confined electrons at the semiconductor surface have recently been studied with growing interest.[1–4]

In a metal-oxide-semiconductor (MOS) structure as shown in Fig. 1, an n-type inversion layer is produced by applying a positive gate voltage V_G on the metal electrode at the surface of a p-type semiconductor. Since the electric field associated with an inversion layer is strong enough to produce a potential well as shown in Fig. 2, the energy levels of the electrons are grouped into "electric subbands,"[2] each of which corresponds to a quantized level for motion in the z direction, with a continuum for motion in the plane parallel to the surface. Within one electric subband, the electrons behave as a two-dimensional electron gas due to the surface quantization effect.

The two-dimensional quantization effect of an

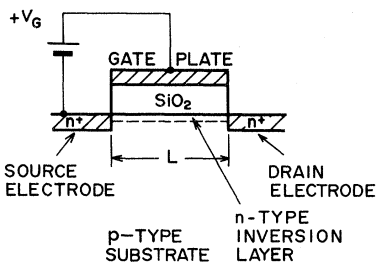

FIG. 1. MOS structure used for the experiment.

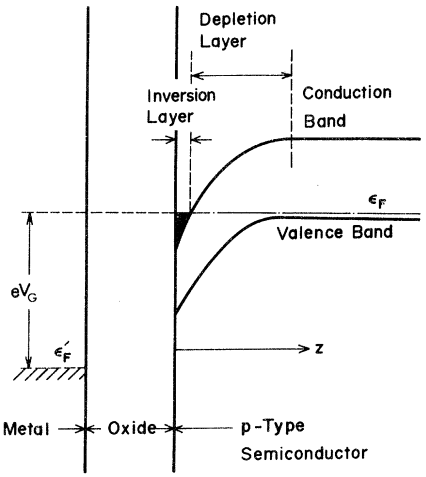

FIG. 2. Energy-band diagram of MOS structure when surface electric field is present.

electron gas in an inversion layer was first observed by Fowler *et al.* in 1966.[5] They observed oscillatory magnetoconductance of n-type inversion layers in a metal-oxide-p-Si structure. The two-dimensional property of the electron gas occupying only one electric subband with the quantum number $n=0$ was also confirmed by their experiments.[6] Since the first observation of the surface quantization effect, much work relating to the electronic structure and the transport properties of electron gas in the inversion layer has been reported.[3,6,7] The direct observations of such quantized levels also have been reported by Tsui[8] with tunneling measurements on a metal-oxide-InAs structure, and additonally by ourselves with measurements of oscillatory magnetoconductance of InSb surface inversion layers.[9,10] In the case of Si surface inversion layers, the energy splitting of electric subbands is larger than the Fermi energy over most of the range of surface electric field available. Therefore, observation of such a quantized level is possible only in one electric subband. However, in the case of a semiconductor with a small effective mass such as InSb, the density of states of the conduction band is small and electrons can populate in higher electric subbands with the moderate strength of the surface electric field. Therefore, many interesting phenomena due to the occupancies of several electric subbands by electrons should be observed.

Prior to the present study, there have been several experiments on the n-type inversion layer of InSb.[11–13] However, the mobilities of specimens used were less than 5×10^3 cm^2/V sec and they were not sufficient for the observation of the Shubnikov–de Haas (SdH)–type oscillations of the conductance. Our samples have shown a mobility larger than 1×10^4 cm^2/V sec, so it has become possible to observe the phenomena due to quantum effects such as SdH-type oscillations.

The principal purpose of this paper is to present experimental evidence for the lowest and the first higher electric subbands of $n=0$ and 1 in n-type inversion layers of InSb surfaces. The transconductance G_m (the differential change of the conductance with respect to the gate voltage V_G) under the magnetic field normal to the surface oscillated as a function of gate voltage V_G. The observed oscillation pattern was found to be composed of two series. The oscillation pattern was compared with one deduced from a theoretical model and good agreement between them was found. So the transconductance maxima were assigned to Landau levels associated with the ground and the first higher electric subbands. Spin splittings were observed above 20 kOe.

II. ELECTRON STATES IN SURFACE INVERSION LAYER

The energy levels of inversion-layer electrons with isotropic effective mass m^* moving in a potential well which depend only on z, the distance from the surface, may be expressed as

$$\epsilon_{n,k_x,k_y}=\epsilon(n)+(\hbar^2/2m^*)(k_x^2+k_y^2), \tag{1}$$

where $\hbar$ is Planck's constant divided by 2π, k_x and k_y are wave vectors, and $\epsilon(n)$ is the energy of one-dimensionally quantized states with quantum number n. The density of states for electrons in the inversion layer, including a factor of 2 for spins, is

$$\rho^{(2)}(\epsilon)=\frac{m^*}{\pi\hbar^2}\sum_n\theta(\epsilon-\epsilon(n)), \tag{2}$$

where $\theta(\epsilon)=1$ if $\epsilon>0$, and $\theta(\epsilon)=0$ otherwise. The energy $\epsilon(n)$ of the surface-quantized states can be obtained by solving the effective mass equation[14] for motion in the potential well of the semiconductor surface.[2,4] By assuming a linear triangular potential well[15,16] for the inversion layer and a simple application of the WKB method,[17] the quantized energy levels are given as

$$\epsilon(n)=\left(\frac{(3\pi e\hbar F_s)^2}{8m^*}\right)^{1/3}(n+\tfrac{3}{4})^{2/3}, \quad n=0,1,2,\ldots \tag{3}$$

where the F_s is the electric field in the inversion layer. The surface electric field is related to the surface electron density n_s as

$$F_s=(4\pi e/\epsilon_s)n_s, \tag{4}$$

where ϵ_s is the dielectric constant of the semiconductor. Thus, the surface electric field F_s controls the electron system through the potential gradient of the inversion layer as well as through the surface carrier density n_s. From Eqs. (2)–(4)

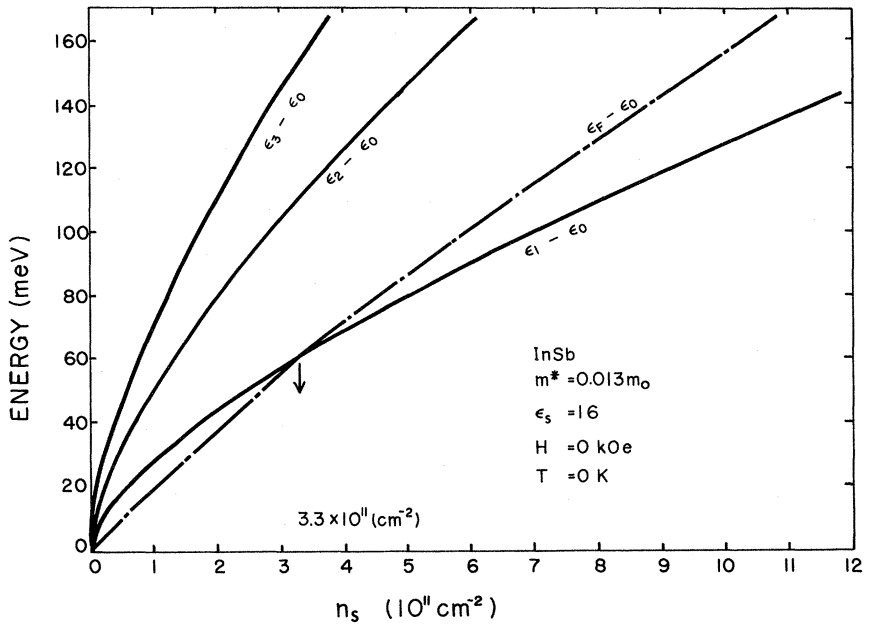

FIG. 3. Energy of the bottom of the electric subbands $\epsilon(n) - \epsilon(0)$ and the Fermi energy $\epsilon_F - \epsilon(0)$ as functions of surface carrier density n_s.

and the Fermi-Dirac distribution function, the quantized energy $\epsilon(n)$ and the Fermi energy ϵ_F were calculated self-consistently as functions of the carrier density n_s for the InSb surface inversion layer where the effective mass of bulk InSb,[18] $m^* = 0.013 m_0$, was used. The use of the bulk effective mass in the surface inversion layer is justified because the surface potential spreads over many unit cells.[19]

In Fig. 3, the bottom of the electric subbands $\epsilon(n)$ and the Fermi level ϵ_F are plotted as a function of n_s where the zero of the energy is set at $\epsilon(0)$. The Fermi level crosses the bottom of the first higher electric subband $\epsilon(1)$ where the carrier density n_s reaches the value of $n_s = 3.3 \times 10^{11}$ cm^{-2}. Electrons occupy both the ground and the first-higher electric subbands above this carrier density.

In a strong magnetic field H, the continua of the energies of the electric subbands become quantized into discrete Landau levels and the energy levels are expressed as

$$\epsilon_{n,l,k_y,s} = \epsilon(n) + (l + \tfrac{1}{2})\hbar\omega_c + sg\mu_B H , \qquad l = 0, 1, 2, \ldots , \quad s = +\tfrac{1}{2}, -\tfrac{1}{2} \quad (5)$$

where $\hbar\omega_c = \hbar eH/m^*c$ is the separation of Landau levels, s the spin quantum number, g the g factor of the conduction electron, and μ_B the Bohr magneton. It should be noted that $\epsilon_{n,l,k_y,s}$ is independent of quantum number k_y and is written as $\epsilon_{n,l,s}$ below. Because the number of states ρ allowed in one Landau level[20] is given by

$$\rho = \tfrac{1}{2}(m^*/\pi\hbar^2)\hbar\omega_c = eH/hc , \quad (6)$$

the density of states for electrons in the inversion layer in a magnetic field is written as

$$\rho_H^{(2)}(\epsilon) = \rho \sum_{n,l,s} \delta(\epsilon - \epsilon_{n,l,s}) \quad (7)$$

in the absence of scattering.[21,22]

The energy levels $\epsilon_{n,l,s}$ and the Fermi level ϵ_F for the InSb inversion layer were calculated as functions of the carrier density n_s, where the g factor of -51 for conduction electrons in the bulk was used.[23] The result of calculation under the magnetic field $H = 20$ kOe is shown in Fig. 4. The notation $0+$, $0-$, $1+$, $1-$, ... indicates the sets of the quantum numbers $(l, s) = (0, +\frac{1}{2})$, $(0, -\frac{1}{2})$, $(1, +\frac{1}{2})$, $(1, -\frac{1}{2})$, ... for the electric subband $n = 0$ and the circled notation indicates the same sets for the subband $n = 1$. As the carrier density n_s is increased, the electrons occupy Landau levels from the lower to the higher. The bold line in Fig. 4 shows the Fermi level at temperature $T = 0$ as a function of the surface carrier density n_s.

While the electrons are occupying the "$\epsilon(0)$ Landau level," the Fermi level in Fig. 4 is expressed by the horizontal lines. When the Fermi level exceeds the value of $\epsilon(1)$, electrons occupy "$\epsilon(1)$ Landau levels" and the Fermi level varies with the $\epsilon(1)$ Landau level as $n_s^{2/3}$. Even after the Fermi level exceeds the value of $\epsilon(1)$, electrons sometimes occupy $\epsilon(0)$ Landau levels and the Fermi level is represented by horizontal lines. The whole tendency of the variation of the Fermi level is similar to the curve in the zero magnetic field. At finite temperatures, the stepwise curve is rounded and the Fermi level varies smoothly with the increasing surface carrier density.

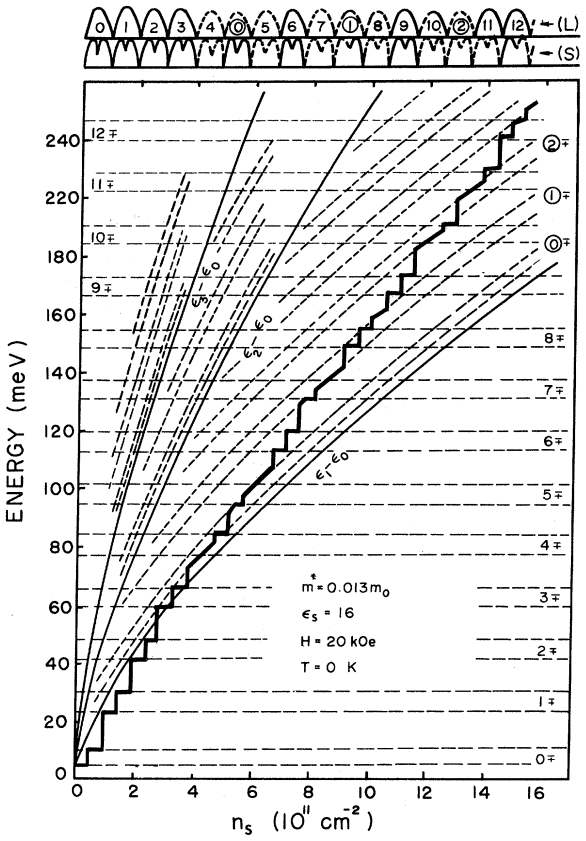

FIG. 4. Energy of the Landau levels $\epsilon_{n,l,s} - \epsilon(0)$ belonging to the electric subbands (dashed lines) and the Fermi level $\epsilon_F - \epsilon(0)$ at $T = 0$ (bold line) as functions of surface carrier density n_s. The Landau quantum numbers are inserted in the figure. The theoretically expected SdH-type oscillations as a function of surface carrier density are inserted in the upper part of the figure. The traces marked (S) and (L) are the oscillation patterns when spin-splitting states are observable and unobservable, respectively.

III. EXPERIMENTAL PROCEDURES

The samples used in the present experiment are insulated-gate field-effect transistors, as shown in Fig. 1, fabricated on single crystals of p-type InSb with the acceptor concentration of about 2×10^{13} cm^{-3}. On the surface of the specimen, silicon dioxide glass, SiO_2, was deposited around 5500 Å, using a chemical-vapor-deposition method in a glow discharge of oxygen gas flow mixed with vapor of tetraethoxysilane. Before the deposition of SiO_2, the (111) B surface of InSb was polished optically flat and etched with a CP-4A solution. Aluminum was evaporated on the glass with the area of 2×3 mm^2 as a gate electrode. To obtain good Ohmic contacts for current electrodes at both sides of the inversion layer, n^+ regions were formed by a technique involving ion implanatation of protons[24] with energies of 200 keV. The source and the drain electrodes were made by soldering with indium-tin alloy on the spots where the insulating oxide layer was removed and rhodium film was electroplated.

Measurements of capacitance C of the MOS structures, surface conductance σ_s, and transconductance G_m of the inversion layer were made as functions of the gate voltage V_G at liquid-helium temperatures. For the SdH-type experiments, magnetic fields were applied by an electromagnet up to 21 kOe and by a superconducting solenoid up to 40 kOe.

The electrical circuit for the capacitance measurements is shown in Fig. 5. An ac signal of a few mV was superposed on the dc gate voltage V_G and the capacitive current was picked up with a small resistor and detected with a lock-in amplifier. In general, the measurements were made at 3.3 kHz, since no dependence on frequency was observed from 30 Hz to 330 kHz.

Measurements of the conductance σ_s and the transconductance G_m were taken simultaneously by the circuit shown in Fig. 6. Measurements were conducted by applying a constant voltage V_{sd} smaller than 0.2 V between the source and drain contacts. The length L of the surface conducting channel was 2 mm and the width W was 3 mm. The drain voltage V_{sd} was kept small enough to avoid hot-electron effects and to ensure uniformity of the surface electric field. In the measurements, the gate voltage V_G was varied slowly so as to keep the electron system in thermal equilibrium, and was swept from negative to positive to avoid the influences of polarization in the oxide layer and charging of the interface states.

The induced charges Q per unit area on the semiconductor surface is related to the surface capacitance[25] as

$$C = dQ/dV_G \,. \tag{8}$$

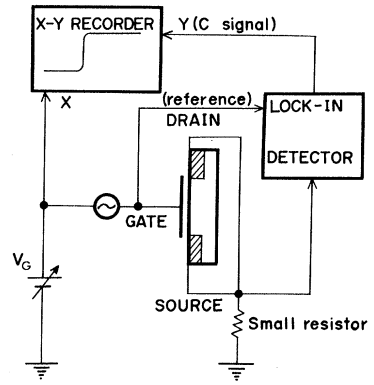

FIG. 5. Circuit for measuring capacitance C as a function of gate voltage V_G.

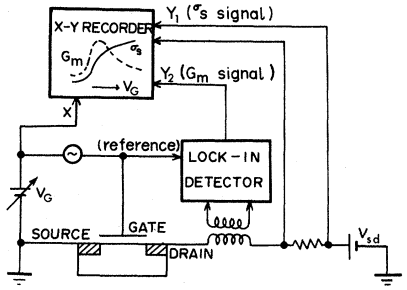

FIG. 6. Circuit for measuring surface conductance σ_s and transconductance G_m as a function of gate voltage V_G under the bias voltage of V_{sd}.

If the trap centers of the carriers or the surface states produced at the interface of the MOS structure are much less than the conduction carriers in the inversion layer, the surface carrier density n_s can be estimated by integrating Eq. (8) as

$$n_s = e^{-1} \int_{-\infty}^{V_G} C(V_G) dV_G \,. \tag{9}$$

The transconductance G_m is the differential conductance with respect to the gate voltage V_G and is written as

$$G_m = \frac{W}{L} V_{sd} \left(\frac{d\sigma_s}{dV_G} \right). \tag{10}$$

Because the mobility μ_s is expressed as $\mu_s = \sigma_s / n_s e$, the G_m can be rewritten as

$$G_m = \frac{WC}{L} V_{sd} \left(\mu_s + n_s \frac{d\mu_s}{dn_s} \right), \tag{11}$$

where the capacitance C is assumed to be constant.

IV. EXPERIMENTAL RESULTS

A. dc Conductivity

A typical result for the measurement of capacitance C and the surface carrier density n_s calculated with Eq. (9) are shown in Fig. 7. The n_s increases with an increase of the gate voltage V_G.[26] The linear dependence of n_s on V_G was assured in most of the specimens above $n_s = 1.0 \times 10^{11}$ cm^{-2}.

Typical results for the measurements of the surface conductance σ_s in the zero magnetic field and in magnetic fields normal to the surface at 4.2 K as a function of the gate voltage are shown in Figs. 8 and 9, respectively. The conductance in magnetic fields displayed SdH-type oscillations with an increase in the surface carrier density n_s. The differentiation of the conductance curves with respect to V_G revealed the clear characteristics of the oscillations; this is given later.

The angular dependence of the conductivity in transverse magnetic fields where the fields were rotated about the axis parallel to the current is shown in Fig. 10. The conductance became minimum when the magnetic field was normal to the surface ($\theta = 0°$). It changed in proportion to $(H \cos\theta)^{-1}$ in the region of $0° < \theta < 60°$. It is seen that the parallel component of the magnetic field is ineffective in comparison with the normal component. However, negative magnetoresistance was observed near the region of $\theta = 90°$, where the bias voltage V_{sd} was set at 1.0 V. Similar tendency has been shown for magnetoresistance of Si surface inversion layers.[27,28]

B. Transconductance

Typical results for the measurement of transcon-

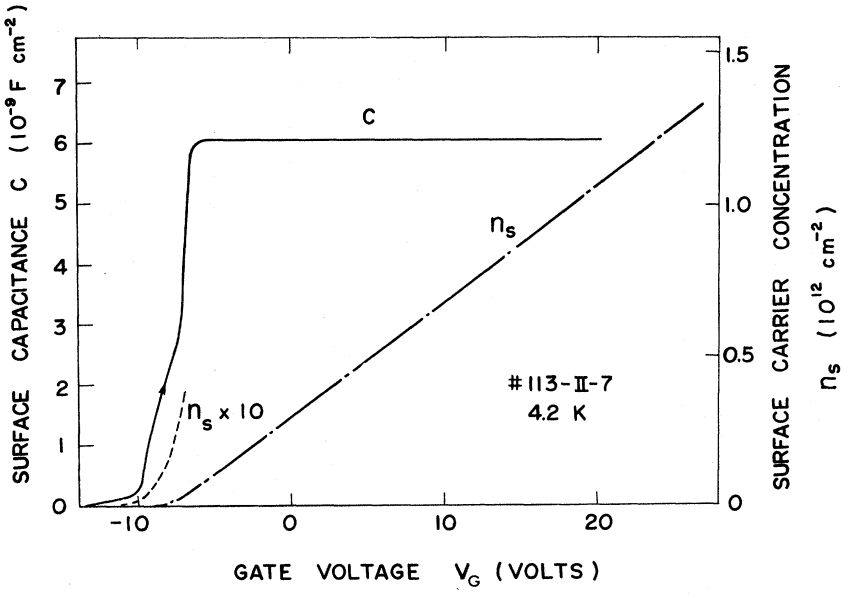

FIG. 7. Measured capacitance C and the surface carrier density n_s calculated from C.

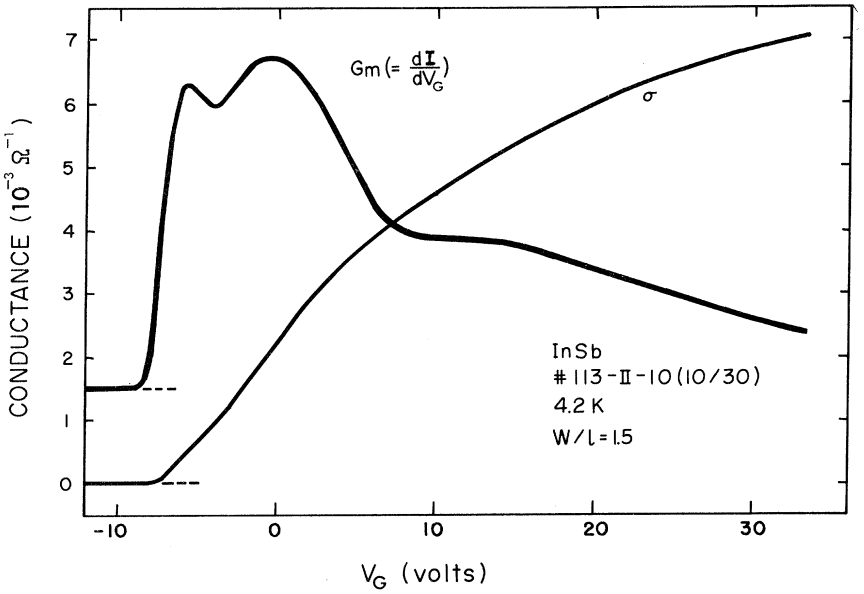

FIG. 8. Measured conductance σ_s and transconductance G_m in zero magnetic field.

ductance G_m in magnetic fields normal to the surface as a function of the gate voltage are shown in Figs. 11(a)–11(c). The result without magnetic field was already shown in Fig. 7, which corresponds to the mobility curve in the sense as mentioned at Eq. (11). The SdH-type oscillations are visible in the wide range of the magnetic fields.

Because the period of the transconductance maxima as a function of V_G was constant, it is presumed that each Landau level contains the same number of states. In the specimen shown in Fig. 11, the

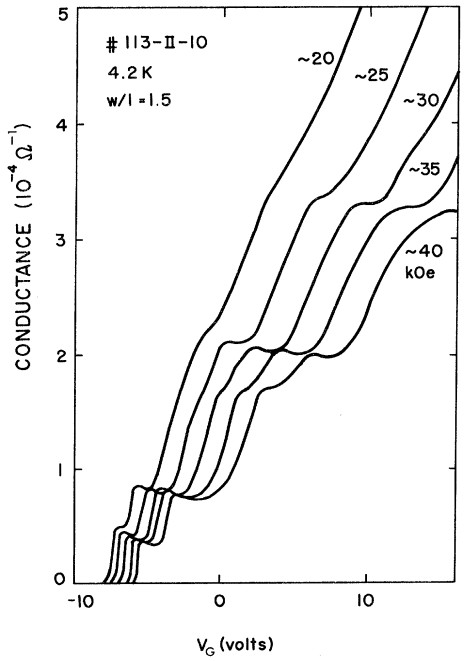

FIG. 9. Variation of the conductance σ_s with magnetic field and gate voltage.

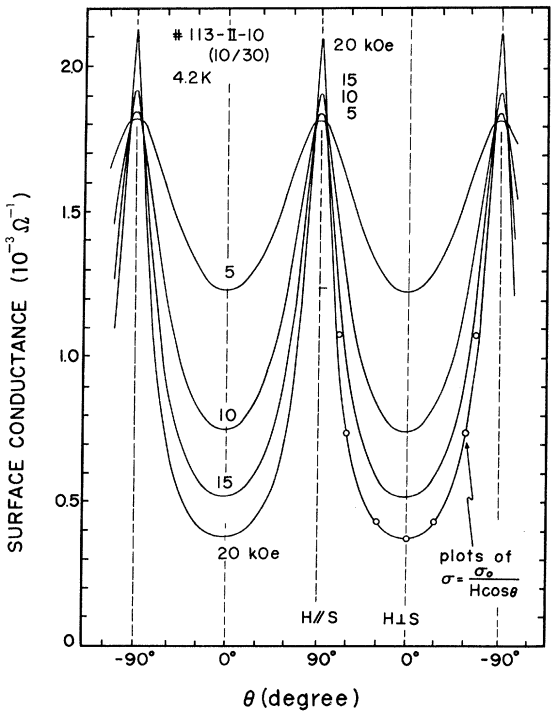

FIG. 10. Angular dependence of surface conductance σ_s, where θ is the angle between the surface normal and the magnetic field. The open circles inserted in the figure are plotted by the equation $\sigma_s = \sigma_0 (H \cos\theta)^{-1}$.

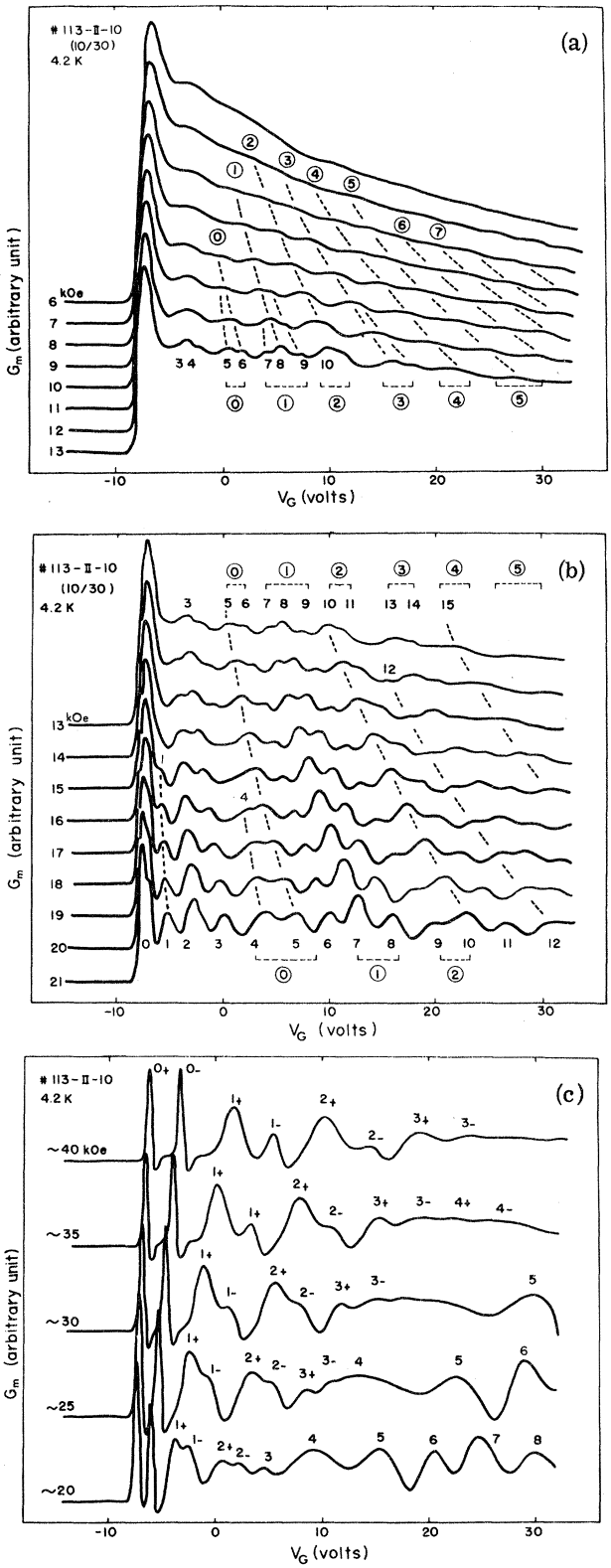

FIG. 11. SdH-type oscillations of transconductance G_m as a function of gate voltage V_G in various magnetic fields. The number inserted at the maxima of the oscillations show the assigned Landau quantum numbers.

surface carrier density n_s varied as $n_s = 4.4 \times 10^{10} (V_G - V_T)$ cm^{-2}, where the threshold voltage for the surface inversion V_T in the specimen was -8 V. The shift of V_T due to the magnetic field was rather small below 20 kOe. Note that the amplitude of the oscillation shows a beating effect, as seen, for example, in Fig. 11(b).

SdH-type oscillations of the conductance were superposed upon the transconductance curve reflecting the surface mobility μ_s, especially in low magnetic fields. Thus the first and second maxima of the oscillation patterns below 10 kOe in Fig. 11 may have a rather different meaning owing to overlapping of the mobility curve.

Gate voltages where the transconductance G_m becomes maximum are plotted against the magnetic field in Fig. 12. The oscillation periods increased as the magnetic field increased. Though the peaks of G_m do not correspond to the peaks of the surface conductance σ_s, we regard the oscillation periods of both quantities as the same. The points in Fig. 12 were connected with an assumption that the similar shapes of the oscillation peaks in Fig. 11 originate from the same Landau levels. Then two groups of lines converging at ϵ_0' and ϵ_1' were obtained as shown in Fig. 12, which indicates that two series of Landau levels do exist.

The transconductance G_m was also measured in a magnetic field tilted up to $\pm 70^\circ$ from the normal to the surface, where the magnetic field was kept at 20 kOe. The oscillation patterns were similar to the curves obtained in the normal-field experiment mentioned above. In Fig. 13, gate voltages at the transconductance maxima obtained in the tilted-field experiment are plotted against the normal component of the magnetic field $H\cos\theta$. The lines drawn in Fig. 13, rather than being those interconnecting the points, are a facsimile of those obtained in Fig. 12. Most of the points lie on the lines. Thus it is concluded that the Landau levels are determined only by the normal component of the magnetic field $H\cos\theta$.[6]

V. SdH-TYPE OSCILLATIONS OF SURFACE INVERSION LAYERS

In an electron gas in the inversion layer in a strong magnetic field normal to the surface, the energy spectrum of the system is completely discrete. In such an ideal system, no type of transport phenomenon should occur, because an infinitesimal amount of energy dissipation required in the electron transport is suppressed by the requirement of energy conservation. Such a system can carry electrical current only with the aid of scatterings.

According to the discussion in Appendix A, the electrical conductivity of such a system is given by

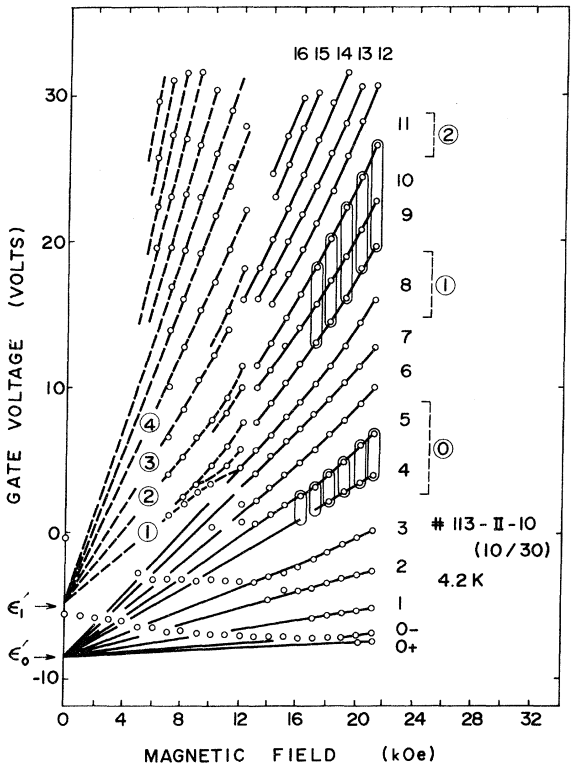

FIG. 12. Gate voltage positions at which the maxima of the transconductance oscillations are observed for the sample of Fig. 11 plotted in various magnetic fields normal to the surface. The two series of Landau levels are shown by solid and dashed lines. The elongated circles indicate the regions where the oscillation amplitudes decrease.

$$\sigma = (e^2/kT)\sum_\nu D_\nu f(\epsilon_\nu)\,[1-f(\epsilon_\nu)]\,, \tag{12}$$

where ϵ_ν denotes the quantized energy $\epsilon_{n,l,s}$, and D_ν is the diffusion coefficient of the orbit center of Landau electrons. From this relation, the conductivity σ was calculated as a function of surface carrier density. In calculation, the density of states of Landau levels is assumed to be a series of δ functions to clarify the dependence of conductivity on surface carrier density. The scatterings are only taken into account in the diffusion constant. Details of the calculation are shown in Appendix B.

When the adjacent Landau levels are separated more than the thermal broadening of the Fermi level, conductivity σ is parabolic as a function of the normalized carrier density $n_s' \equiv n_s/\rho$ and becomes maximum near $\epsilon_F = \epsilon_\nu$; i.e., n_s' = integer $+\frac{1}{2}$. In Fig. 14, we considered two Landau levels denoted by ϵ_A' and ϵ_B' taking zero of the energy as $\epsilon(0)$. Here, we introduce the reduced conductivity η,

$$\eta = \sum_\nu f(\epsilon_\nu)\,[1-f(\epsilon_\nu)]\,, \tag{13}$$

where the diffusion constants D_ν are assumed to be the same at the two levels. As shown in Appendix B, η takes maxima at near $n_s' = \frac{1}{2}$ and $\frac{3}{2}$ if $\epsilon_A' - \epsilon_B' > 2.6kT$; if not, it takes a maximum at $n_s' = 1$. The latter is due to thermal broadening of the Fermi level. In the above, $\epsilon_\nu' = \epsilon_\nu - \epsilon(0)$ is taken to be constant because we considered the Landau levels ϵ_ν belonging to the ground electric subband $\epsilon(0)$. In Fig. 15, we considered the case where a Landau level A is associated with an $\epsilon(0)$ electric subband and a Landau level B is associated with an $\epsilon(1)$ electric subband. The energy ϵ_B' increases in proportion to $n_s'^{2/3}$ and overtakes the energy ϵ_A' at the carrier density n_{s0}'. Then, the expected two maxima generally come close to each other and the reduced conductivity maxima are broadened. The oscillation amplitude decreases in this case.

The pattern of SdH oscillation can be obtained from variation of the Fermi level in Fig. 4, based on the above consideration. In the upper part of

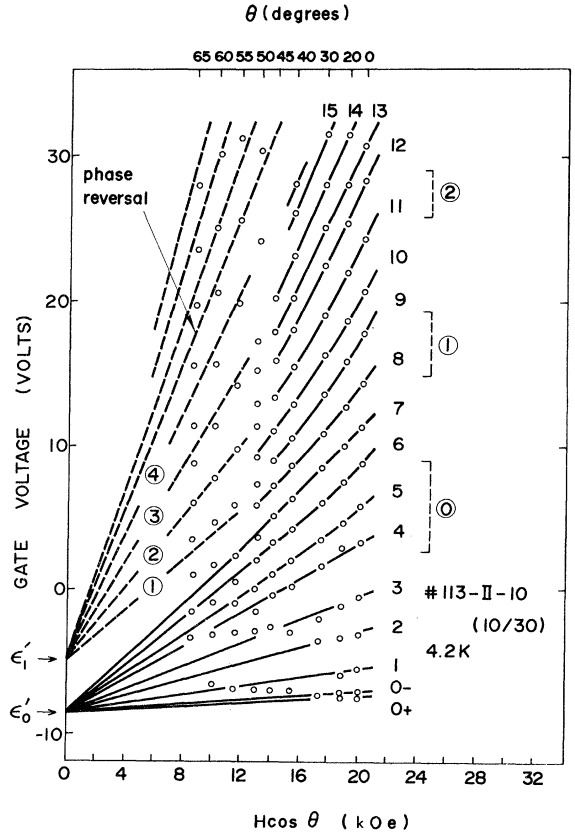

FIG. 13. Same as Fig. 12 except that the magnetic field is kept at 20 kOe and tilted up to 70° from the normal to the surface. The tilted angle θ is shown in the upper part of the figure.

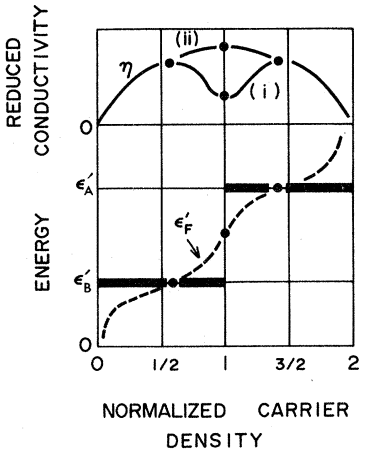

FIG. 14. Illustration of the reduced conductivity as a function of the normalized surface carrier density n'_s in case (2) in Appendix B. The Fermi level ϵ'_F and the Landau levels ϵ'_A and ϵ'_B as functions of n'_s are shown. Bold line is the Fermi level at $T=0$.

Fig. 4, the schematic curves of SdH oscillations are shown. In these patterns, we discriminate between the peaks originating in $\epsilon(0)$ Landau levels and those originating in $\epsilon(1)$ Landau levels by using solid lines and dashed lines, respectively. In the upper pattern marked (L), spin splitting is neglected. The coalescence of spin-split maxima will occur when the level broadening is much larger than the spin splitting, as well as when the two levels draw near and break the condition $\epsilon_A - \epsilon_B > 2.6kT$. The number inserted in the pattern represents the Landau quantum number l. In Fig. 4, we have a case where the level crossings occur as shown in Fig. 15. In this case, the oscillation pattern becomes nonparabolic and broadened. The oscillation amplitude is expected to become small near the level-crossing region. This phenomenon may well be regarded as interference of the Landau levels of the different electric subbands.

VI. DISCUSSION

A. Evidence of Surface Quantization

The surface-quantization effect would be washed out if electrons suffered frequent scatterings.[29] The Landau quantization effect would also be smeared out if the Landau electrons were scattered frequently in one cycle of the cyclotron motion. Thermal disturbance also prohibits observation of the quantized states. Thus, the following conditions are required to observe these quantization effects:

$$\epsilon(1) - \epsilon(0) > \hbar/\tau, kT , \tag{14}$$

$$\hbar\omega_c > \hbar/\tau, kT , \tag{15}$$

where kT is the thermal energy and τ^{-1} is the collision frequency.

To estimate the collision broadening of the quantum levels, we calculate the τ^{-1} from the mobility measured. The mobility in zero magnetic field was $\mu_s = 1\times10^4$ cm^2/V sec and the temperature $T = 4.2$ K; thus, $\hbar/\tau = 7$ meV and $kT = 0.36$ meV. Since $\epsilon(0)$ and $\epsilon(1)$ are of the order of 10–100 meV, as discussed below, condition (14) is well satisfied. Condition (15) will be satisfied for magnetic fields above 5 kOe. From the g factor of -51 for the conduction electrons in the bulk,[23] the spin splitting of InSb is estimated to be $0.36\hbar\omega_c$; thus, for observing spin splitting, stronger magnetic fields are needed.[30]

The order number corresponding to the series of the oscillation maxima shown in Fig. 11 was plotted in Fig. 16 as a function of the gate voltage. Well-defined oscillation peaks were observed above 10 kOe for every sample that we measured. Figure 16 confirms that the oscillation period is constant. The oscillation period also changed linearly with increasing the magnetic field strength as shown in Fig. 12.

From the experimental results, it is possible to determine the number of states of electrons which fill up one Landau level in the InSb surface inversion layer. From the same procedures as shown in Fig. 16, we can determine the oscillation periods of the gate voltage (ΔV_G/order) and the carrier densities (Δn_s/order). According to Eq. (6), the number of the states in each Landau level is given by

$$\Delta n_s/\text{order} = 2.4\times10^9 g_d H \text{ cm}^{-2} , \tag{16}$$

where g_d shows the degeneracy factor of the Landau level and H is measured in unit of kOe. Combining the experimentally determined period with Eq. (16), we determined the level degeneracy g_d for all the

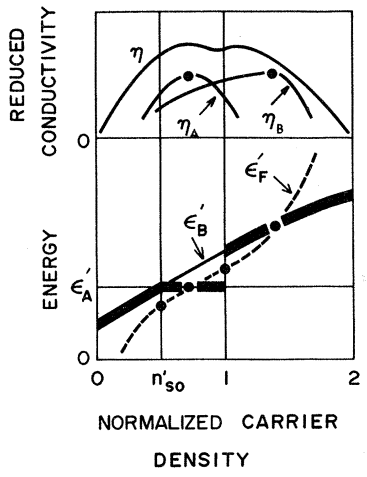

FIG. 15. Illustration of the reduced conductivity; same as Fig. 14 in case (3) in Appendix B.

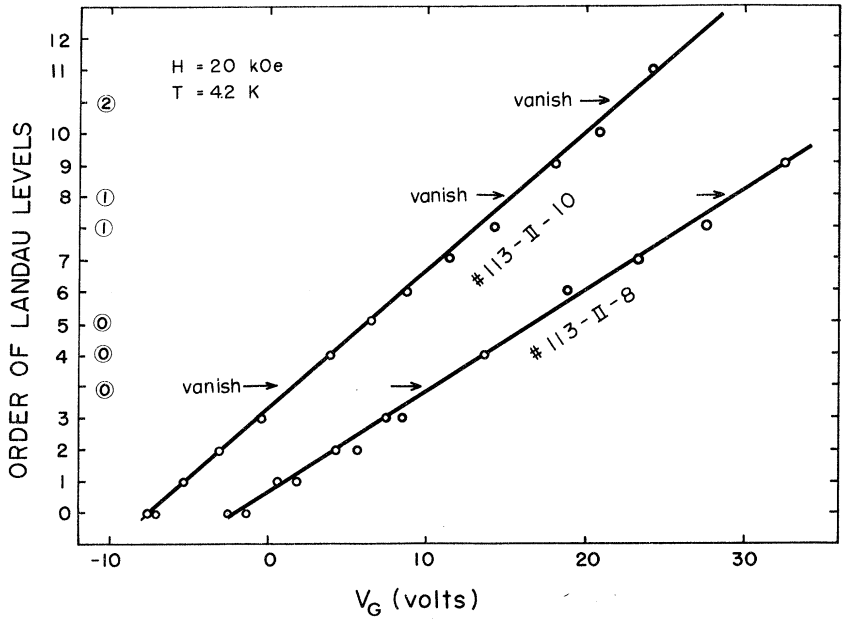

FIG. 16. Order numbers of the oscillation maxima observed for two different samples in a magnetic field $H = 20$ kOe plotted as a function of the gate voltage positions at which the oscillation maxima occur. The numbers inserted along the ordinate are the assigned Landau quantum numbers according to the theory discussed in the text.

samples measured. The degeneracy factor g_d thus determined is 2.0 ± 0.2, which is reasonably ascribed to the spin degeneracy of the Landau levels. This result indicates that it is difficult to observe the effects of spin splitting in conductance oscillation in the range 13–21 kOe shown in Fig. 11(b) because of the broadening of Landau levels. However, in strong magnetic fields above 20 kOe, the same oscillation maximum splits into a pair of peaks as seen in Fig. 11(c). The spin splitting is clearly evident in Figs. 11(c) and Fig. 16.

B. Two Series of Landau Levels

Referring to the curves as shown in Fig. 4, we plotted the surface carrier density calculated theoretically where the maximum of the conductance should occur in the different magnetic fields in Fig. 17. In calculation, the inversion-layer potential was assumed to be linear, as discussed in Sec. II. Connecting the points belonging to the same Landau quantum numbers, two groups of lines intersecting the abscissa at $n_s = 0$ and $n_s = 3.3 \times 10^{11}$ cm^{-2} are obtained. The intersection point at $n_s = 3.3 \times 10^{11}$ cm^{-2} corresponds to the onset of occupancy of the first higher electric subband $n = 1$ with electrons. It is observable that the calculated curve (Fig. 17) closely approximates the curves obtained from the experiments (Figs. 12 and 13). Assignment of the Landau levels is easily made as shown in Figs. 11–13.

From Fig. 12 is obtained the difference of the gate voltage ΔV_G between the points ϵ_0' and ϵ_1'. From ΔV_G, the surface carrier density Δn_s at which the Fermi level ϵ_F meets the bottom of the higher electric subband $n = 1$ can be calculated. The quantity $(m^*/m_0)[\epsilon(1) - \epsilon(0)]$, which is proportional to Δn_s, was estimated. The values of $\epsilon(1) - \epsilon(0)$ obtained from experimentally determined Δn_s and the effective mass of $m^* = 0.013 m_0$ were one-half or one-third the value calculated under the assumption of the linear triangular potential well with the surface carrier density $n_s = 3.3 \times 10^{11}$ cm^{-2} (Fig. 3). The

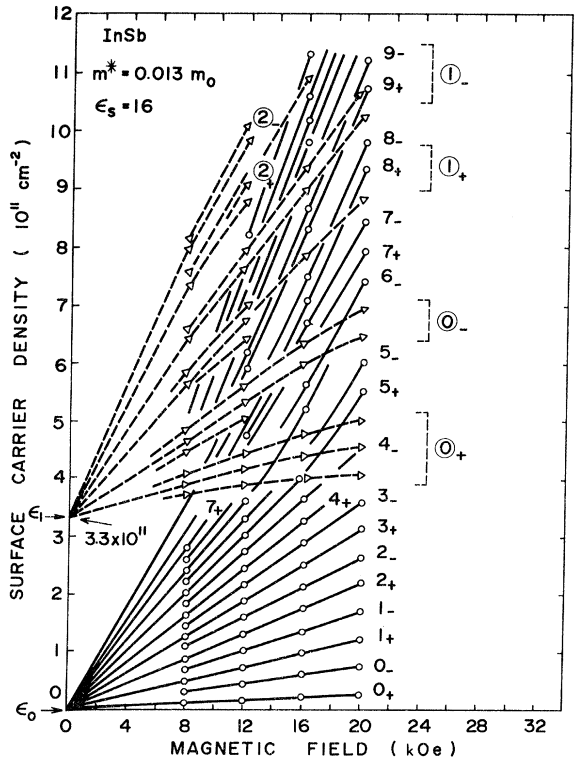

FIG. 17. Surface carrier densities at which the conductivity maxima of SdH-type oscillations occur plotted theoretically in different magnetic fields.

TABLE I. Occupation order of Landau levels (theoretical). Landau quantum numbers l are listed here as 0, 1, 2, ... for $\epsilon(0)$ Landau levels ($n=0$) and 0, ①, ②, ... for $\epsilon(1)$ Landau levels ($n=1$). Parenthesized terms indicate the simultaneous occupation of two Landau levels (see text).

$H=12$ kOe	0, 1, ..., 5, 6, (0, 7), 0, (0, 8), 9, (①, 10), ①, (①, 11), 12, (②, 13), ②, ...
$H=16$ kOe	0, 1, 2, 3, 4, (0, 5), 0, 6, 7, 8, ①, (①, 9), 10, 11, ...
$H=20$ kOe	0, 1, 2, 3, (0, 4), (0, 4), (0, 5), 6, 7, ①, (①, 8), 9, 10, ②, 11, 12, ...

discrepancy by a factor of 2 or 3 between the experiment and the theory might be due to difficulty of the SdH measurement in weak magnetic fields and also due to roughness of the linear-potential assumption. This assumption is possible when the Coulomb potential associated with electrons in the inversion layer is neglected in comparison with the potential due to the external field applied on the surface. Before the Fermi level reaches the bottom of the higher electric subband, the lowest subband is occupied by many electrons.

The linear-potential approximation is inadequate, especially for the higher electric subband, because the electron wave function of the higher subband is more spread out, than that of the lowest subband. Howard[2] and Stern[22,31] calculated the energy of the electric subbands with a self-consistent surface potential by solving the coupled equation of the Poisson and Schrödinger equations. According to the self-consistent calculation by Howard,[2] the ground-state energy $\epsilon(0)$ is reduced to 80% of that calculated from the linear-potential assumption, and the energy difference $\epsilon(1)-\epsilon(0)$ becomes about 30% in a special case of Si(100) surface. In the case of InSb, the situation might be the same. Thus, the discrepancy in energy difference between the theory and the experiment in our case might be due to roughness of the linear-potential assumption.[32]

C. Effect of Higher Electric Subband on SdH-Type Oscillations

The lines interconnecting the points in Fig. 12 bend superlinearly in the high-V_G region. This fact is also seen in Fig. 17, the diagram obtained theoretically. This is due to a slowdown of the filling rate of electrons for each electric subband in this region where electrons occupy both the ground and the higher electric subbands, and the Fermi level increases more slowly.

Referring to the pattern of the SdH oscillation marked (L) in Fig. 4 where the spin-splitting was unobservable, we tabulated the "occupation order" of electrons into the Landau levels in Table I. The parenthesized terms express that the electrons have to occupy both Landau levels in the parentheses simultaneously, even at $T=0$, where broadened maxima of the SdH oscillation are expected as shown in Fig. 15. In comparison with the occupation order in Table I, we can put the Landau quantum numbers into the ordinate of Fig. 16. Here we see the coincidence of the vanished peaks to the $\epsilon(1)$ Landau levels, even in different samples. The skipping of the oscillation maxima and the decreased amplitude of the oscillations in Figs. 11(b) and 11(c) are due to simultaneous occupation of the two Landau levels.

In magnetic fields below 12 kOe, we observed a long period of oscillations among the levels marked by the circled numbers in Figs. 12 and 11(a). Theoretically, no simple oscillation maxima are expected in such weak magnetic fields because separation of the Landau levels $\hbar\omega_c$ is comparable to or smaller than the broadening of the levels $\Gamma\sim 10$ meV. As seen in Fig. 12, the oscillation period in 6 kOe is comparable to that in 18 kOe. The oscillation in 6 kOe belongs to the higher electric subband $\epsilon(1)$, and the oscillation in 18 kOe belongs to the ground electric subband $\epsilon(0)$. The result means that while the oscillation period in 18 kOe is 2ρ, the oscillation period in 6 kOe is 6ρ because ρ itself is three times larger in 18 kOe than that in 6 kOe. Theoretically, the fundamental period of $\epsilon(0)$ Landau levels is ρ when spin splitting is included, but that of $\epsilon(1)$ Landau levels is five to six times larger,[9] as seen in Fig. 17. This is caused by oscillation maxima which enter those which belong to another series of Landau levels. Thus the experimental long-period oscillation shown in Fig. 11(a) is attributed to the modulation of the fundamental oscillations by the $\epsilon(1)$ Landau levels.

D. Spin-Splitting States

The experimental oscillation maxima assigned to the spin-splitting states occur in pairs in the oscillation patterns shown in Fig. 11(c), while an elementary theory predicts equal spacings of the oscillation maxima. This pairing may be attributed to the effect of a finite temperature T which causes broadening of the Fermi level: Electrons must occupy two Landau levels simultaneously; thus, more electrons are needed in order that the Fermi level can reach the lower Landau level of the two in question, as already explained in Fig. 14 of Sec. V and in Appendix B.

The oscillation period in tilted magnetic fields shown in Fig. 13 indicates that the existence of the parallel component of the magnetic field $H\sin\theta$ is negligible. Moreover, in the dc conductance measurement as in Fig. 10, the conductivity in transverse magnetic fields varied in proportion to $(H\cos\theta)^{-1}$. On the other hand, the resistance in magnetic fields normal to the surface varied linearly with the magnetic field strength H shown in Fig. 18, where SdH-type oscillations were blurred.

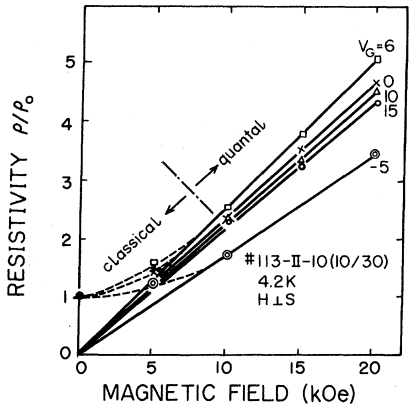

FIG. 18. Normalized resistivity as a function of magnetic field normal to the surface with the gate voltage as a parameter.

Both data reveal that only the normal component of the magnetic field $H\cos\theta$ was effective in the conductance measurements. Thus, it is confirmed experimentally that the Landau quantization is caused only by $H\cos\theta$.

When the magnetic field is tilted at an angle θ from the normal to the surface, the spin splitting belonging to each Landau level may be assumed to be determined by the total magnetic field H, while the Landau quantization was caused only by the normal component $H\cos\theta$. At a certain tilted angle $\theta=\theta_0$, the spin splitting $g\mu_B H$ becomes equal to the Landau level separation $\hbar\omega_c$, and the levels of the different Landau quantum numbers have the same energy. If we increase the Fermi energy in such a situation, the oscillation maxima arise at points where the Fermi level meets the duplicated Landau level. If we apply the magnetic field of $H\cos\theta_0$ normally to the surface, the oscillation maxima occur in the middle of the two Landau levels with the same Landau quantum number l when broadening of the levels is present. Thus, the oscillations will be out of phase in both cases.[6] The phase reversal is evident in the experimental data shown by the arrow in Fig. 13. From Fig. 13, we assume $\theta_0=65°-70°$. Then the spin-splitting factor g is estimated from

$$(m^*/m_0)g=2\cos\theta_0\,. \tag{17}$$

Experimentally, we have obtained the value of $2\cos\theta_0$ as 0.76 ± 0.1. If we use the values of $m^*=0.013m_0$ and $g=-51$, the parameters of the bulk InSb, then the value of $2\cos\theta_0$ is 0.66.

VII. CONCLUSION

Shubnikov–de Haas-type oscillations of an electron gas with discrete energy levels confined in n-type inversion layers of InSb surfaces have been studied. Two series of oscillations have been observed which correspond to the series of Landau levels associated with the ground and the first higher electric subbands. Two-dimensional property of the electron gas was confirmed by quantitative analysis of the number of states of a discrete Landau level. The observed Landau levels could be assigned in comparison with a theoretical model deduced from the linear-potential assumption in the inversion layer. This model explains the oscillation of the magnetoconductance caused by a change of the surface electric field.

ACKNOWLEDGMENTS

We express our sincere gratitude to Professor H. Kawamura of Osaka University for his many valuable discussions and encouragement throughout this work. We are also grateful to Y. Murayama for his stimulating discussions and to T. Shimada and Y. Shiraki for their ion implantation of H^+ into InSb for Ohmic contacts formation.

APPENDIX A: ELECTRICAL CONDUCTIVITY OF ELECTRON GAS IN STRONG MAGNETIC FIELD

The Landau states do not have an average velocity perpendicular to the magnetic field, since the velocity operator has no diagonal matrix elements. The nondiagonal part of the density matrix in the Liouville equation is required to describe the electric current carried by the Landau electrons. The second-order perturbational treatment of the Liouville equation with respect to the scattering potential[33] gives the following expression for the conductivity σ:

$$\sigma=-e^2\sum_\nu D_\nu\left(\frac{df}{d\epsilon}\right)_{\epsilon=\epsilon_\nu} \tag{A1}$$

$$=-e^2\int D_\nu(\epsilon_\nu)\left(\frac{df}{d\epsilon}\right)_{\epsilon=\epsilon_\nu}\rho(\epsilon_\nu)d\epsilon_\nu\,, \tag{A2}$$

$$D_\nu=\sum_\mu \tfrac{1}{2}W_{\mu,\nu}(X_\mu-X_\nu)^2\,, \tag{A3}$$

$$W_{\mu,\nu}=(2\pi/\hbar)\,|M_{\mu,\nu}|^2\delta(\epsilon_\mu-\epsilon_\nu)\,, \tag{A4}$$

$$M_{\mu,\nu}=\langle\mu|v|\nu\rangle\,, \tag{A5}$$

where f is the Fermi-Dirac distribution function and $\rho(\epsilon)$ is the density of states for a Landau electron. μ and ν are quantum numbers which denote the quantum states. D_ν is the diffusion coefficient, X_ν the cyclotron-orbit center,[34] $W_{\mu,\nu}$ the transition probability, $M_{\mu,\nu}$ the matrix element, and v the scattering potential. X_ν is equal to $-l_c^2 k_y$, where l_c is the classical radius of a Landau orbit and k_y the wave vector perpendicular to the magnetic field. The expression indicates that the current is brought about by jumps of the cyclotron-orbit centers X_ν caused by a certain scattering potential v. Equation (A1) is rewritten as

$$\sigma=(e^2/kT)\sum_\nu D_\nu f(\epsilon_\nu)[1-f(\epsilon_\nu)]\,. \tag{A6}$$

If scattering centers with a δ-function-type short-range force are distributed randomly, the scattering potential is expressed as

$$v = a \sum_{i}^{N_I} \delta(\vec{r} - \vec{r}_i) , \tag{A7}$$

where $\vec{r}_i$ and N_I denote the position and the number of the scattering centers, respectively. Then, a simple calculation for the conductivity caused only by the ground-state Landau level ($l = 0$) gives

$$\sigma = \frac{e^2 a^2 N_I}{16 \pi^3 \hbar l_c^2} \left(-\frac{df}{d\epsilon}\right)_{\epsilon=\epsilon_{l=0}} , \tag{A8}$$

where the density of states of the Landau level is approximated by Eq. (7) in the text and the wave function by an Airy function.[35]

APPENDIX B: CALCULATION OF SdH-TYPE OSCILLATIONS AS FUNCTION OF SURFACE CARRIER DENSITY

One or two Landau levels are considered here for convenience of the calculation. The normalized surface carrier density n_s' is varied from 0 to 1 or 2 corresponding to the number of Landau levels.

Case (1): Only one Landau level is occupied ($\nu = A$). If only one Landau level is contained in the energy range where the value of $df/d\epsilon$ is not zero, the conductivity is expressed as

$$\sigma = (e^2/kT) D_A n_s' (1 - n_s') . \tag{B1}$$

The oscillation pattern is parabolic and σ is maximum when the level is exactly half occupied. The Fermi level is obtained as

$$\epsilon_F = \epsilon_A - kT \ln\left(\frac{1 - n_s'}{n_s'}\right) . \tag{B2}$$

The Fermi level varies from $-\infty$ to $+\infty$ when n_s' varies from 0 to 1. At the maximum of σ, $\epsilon_F = \epsilon_A$.

Case (2): Two Landau levels are occupied ($\nu = A, B$). We assume that $\epsilon_A - \epsilon_B$ is positive and not changed by increasing n_s, and that the diffusion coefficients of the adjacent Landau levels are not much different; thus

$$D_A \approx D_B . \tag{B3}$$

Then, the conductivity σ is

$$\sigma \approx (e^2/kT) D_A \eta , \tag{B4}$$

where

$$\eta = \textstyle\sum_\nu f(\epsilon_\nu)[1 - f(\epsilon_\nu)] . \tag{B5}$$

The calculated result is as follows.

(i) $\epsilon_A - \epsilon_B > 2.6kT$: η takes maxima at $n_s' = 1 \pm \frac{1}{2} (\beta - 1)^{-1} (\beta^2 - 14\beta + 1)^{1/2}$ and takes a minimum at $n_s' = 1$, where

$$\beta = e^{(\epsilon_A - \epsilon_B)/kT} ; \tag{B6}$$

(ii) $0 < \epsilon_A - \epsilon_B \leqq 2.6kT$: η takes a maximum at $n_s' = 1$.

The conductivity takes two maxima when the two Landau levels are well separated. The two maxima come closer to each other when the temperature T becomes higher. In the latter case, the two maxima coalesce into a maximum owing to thermal broadening of the Fermi level. This situation is shown in Fig. 14. The following inequality explains the proximity of the two peaks at higher temperatures:

$$\left| \tfrac{1}{2} (\beta - 1)^{-1} (\beta^2 - 14\beta + 1)^{1/2} \right| < \tfrac{1}{2} . \tag{B7}$$

Case (3): Two Landau levels are occupied where the level crossing occurs ($\nu = A, B$). We shall consider the case where the energy ϵ_B increases and overtakes the energy ϵ_A at the carrier density n_{s0}'. The two Landau levels degenerate at $n_s = n_{s0}$. For simplicity, we assume Eq. (B3) in this case. Then, the conductivity is

$$\sigma \approx (e^2/kT) D_A \eta , \tag{B8}$$

$$\eta = \eta_A + \eta_B , \tag{B9}$$

$$\eta_A = f(\epsilon_A)\,[1 - f(\epsilon_A)] , \tag{B10}$$

$$\eta_B = f(\epsilon_B)[1 - f(\epsilon_B)] . \tag{B11}$$

The conductivity σ as a function of n_s' is analyzed as follows.

(i) $0 < n_{s0}' < 1$. Since conductivity depends on the energy separation between the Landau levels and the Fermi level, we follow the variation of the Fermi level when the carrier density is increased. As shown in Fig. 15, the Fermi level passes through the point just below the level-crossing point at $n_s' = n_{s0}'$ and also passes through the mean point of the two levels at $n_s' = 1$. The bold line in Fig. 15 is the Fermi level at $T = 0$. At a finite temperature, the curve becomes rounded off as shown by dashed lines. Thus, curves η_A, η_B, and η can be drawn. It should be noted that η is asymmetrical about the line $n_s' = 1$ and has two broad peaks. This broadness is due to the fact that η_B has a small hump or shoulder in the region of $n_s' < 1$, and that the two peaks are close together.

(ii) $1 < n_{s0}' < 2$. The situation is the same as above.

(iii) $n_{s0}' = 1$. The two Landau levels become degenerate at $n_s' = 1$. Both η_A and η_B have maxima at the point and the curve η is symmetrical about the line where $n_s' = 1$. The height of the peak is twice that of the η_A or η_B peak.

[1] F. F. Fang and W. E. Howard, Phys. Rev. Letters 16, 797 (1966).

[2] F. Stern and W. E. Howard, Phys. Rev. 163, 816 (1967).

[3] F. F. Fang and A. B. Fowler, Phys. Rev. 169, 619 (1967).

[4] E. D. Sigga and P. C. Kwok, Phys. Rev. B 2, 1024 (1970).

[5]A. B. Fowler, F. F. Fang, W. E. Howard, and P. J. Stiles, Phys. Rev. Letters 16, 901 (1966); J. Phys. Soc. Japan Suppl. 21, 331 (1966).

[6]F. F. Fang and P. J. Stiles, Phys. Rev. 174, 823 (1968).

[7]A. F. Tasch, Jr., D. D. Buss, R. T. Bate, and B. H. Breazeale, in Proceedings of the International Conference on the Physics of Semiconductors, Boston, 1970, p. 458 (unpublished).

[8]D. C. Tsui, Phys. Rev. Letters 24, 303 (1970).

[9]Y. Katayama, N. Kotera, and K. F. Komatsubara, in Ref. 7, p. 464.

[10]Y. Katayama, N. Kotera, and K. F. Komatsubara, Japan. J. Appl. Phys. Suppl. 40, 214 (1970).

[11]S. Kawaji, H. Huff, and H. C. Gatos, Surface Sci. 6, 234 (1967); S. Kawaji and H. C. Gatos, *ibid.* 6, 362 (1967).

[12]K. F. Komatsubara, H. Kamioka, and Y. Katayama, J. Appl. Phys. 40, 2940 (1969).

[13]K. F. Komatsubara, Y. Katayama, N. Kotera, and T. Kobayashi, J. Vac. Sci. Technol. 6, 572 (1969).

[14]L. M. Luttinger and W. Kohn, Phys. Rev. 97, 869 (1965).

[15]A. Kobayashi, Z. Oda, S. Kawaji, H. Arata, and K. Sugiyama, J. Phys. Chem. Solids 14, 37 (1960).

[16]S. Kawaji and H. C. Gatos, Surface Sci. 7, 215 (1967).

[17]The accuracy of this approximation is within 0.7% even in the worst case of $n=0$.

[18]O. Madelung, *Physics of III-V Compounds* (Wiley, New York, 1964), pp. 53, 76, 90, and 101.

[19]The spreads of the electron wave functions z_s from the surface estimated from the classical turning points of the potential edge are $z_s=147(n_s/10^{12})^{-1/3}$ Å for $n=0$ state and $z_s=260(n_s/10^{12})^{-1/3}$ Å for $n=1$ state.

[20]C. Kittel, *Quantum Theory of Solids* (Wiley, New York, 1963), p. 219.

[21]When the appropriate level broadenings are taken into account, the δ function may be replaced by a Lorentzian or a more complicated function. See Ref. 22 and K. Ohta, Japan. J. Appl. Phys. 10, 850 (1971).

[22]F. Stern, in Ref. 7, p. 451.

[23]G. Bemski, Phys. Rev. Letters 4, 62 (1960). M. Gueron, in *Proceedings of the Seventh International Conference on the Physics of Semiconductors, Paris,* 1964 (Academic, New York, 1965), p. 433; K. F. Komatsubara, Phys. Rev. Letters 16, 1044 (1966); R. A. Issacson, Phys. Rev. 169, 312 (1968).

[24]A. G. Foyt, W. T. Lindley, and J. P. Donnelly, Appl. Phys. Letters 16, 335 (1970).

[25]A. Many, Y. Goldstein, and N. B. Grover, *Semiconductor Surfaces* (North-Holland, Amsterdam, 1965), p. 221.

[26]The capacitance curves measured at 300 Hz did not change even in a strong magnetic field except for a shift due to shift of the band edge caused by the Landau quantization. Anomalous dips in the capacitance curve reported by Kaplit and Zemel were not found [M. Kaplit and J. N. Zemel, Phys. Rev. Letters 21, 212 (1968)]. Though we found a similar series of dips, they disappeared with decreasing frequency. The results indicated that the observed dips did not result from the capacitive current but from the resistive current because the component of the capacitive current increased as the frequency was lowered in our measuring circuit.

[27]S. Tansal, A. B. Fowler, and R. F. Cotellesa, Phys. Rev. 178, 1326 (1969).

[28]Y. Uemura and Y. Matsumoto, J. Japan. Soc. Appl. Phys. Suppl. 40, 205 (1971).

[29]J. R. Schrieffer, in *Semiconductor Surface Physics*, edited by R. H. Kingston (Pennsylvania U. P., Philadelphia, 1957), p. 55.

[30]Stern has argued in Ref. 22 that the energy broadening parameter Γ enters in the amplitude of conductance oscillations through the factor $\exp(-2\pi\Gamma/\hbar\omega_c)$. The Γ estimated from the oscillation amplitudes in different magnetic fields (15–21 kOe) was the order of 10 meV, where the bulk effective mass of $m^*=0.013m_0$ was used. Though the value Γ should be the sum of kT and $\hbar/2\tau$, the latter term was dominant here. This was consistent with the fact that the oscillation amplitudes did not differ greatly at 1.5 and 4.2 K.

[31]F. Stern, J. Comput. Phys. 6, 56 (1970).

[32]Increase of the electron effective mass with the electron concentration (O. Madelung, Ref. 18, pp. 86 and 95) also causes the energy difference $\epsilon(1)-\epsilon(0)$ to decrease. However, as the density of states of the band is more strongly increased by nonparabolicity, the expected Δn_s of the quantity $(m^*/m_0)[\epsilon(1)-\epsilon(0)]$ increases by the degree of nonparabolicity.

[33]A. H. Kahn and H. P. R. Frederikse, in *Solid State Physics*, edited by F. Seitz and D. Turnbull (Academic, New York, 1959), Vol. 9, p. 270; P. N. Argyres and L. M. Roth, J. Phys. Chem. Solids 12, 89 (1959); E. N. Adams and T. D. Holstein, *ibid.* 10, 254 (1959); L. M. Roth and P. N. Argyres, in *Semiconductors and Semimetals*, edited by R. K. Willardson and A. C. Beer (Academic, New York, 1966), Vol. 1, p. 159.

[34]R. Kubo, S. Miyake, and N. Hashitsume, in *Solid State Physics*, edited by F. Seitz and D. Turnbull (Academic, New York, 1965), Vol. 17, p. 276.

[35]For example, see the paper in Ref. 21.